

## Research Article

# Optimization of Convective Tray-Drying Process Parameters for Green Banana Slices Using Response Surface Methodology and Its Characterization

Meenatai Kamble <sup>1</sup>, Anurag Singh <sup>1,2</sup>, Sukh Veer Singh <sup>1</sup>, Ajay Chinchkar <sup>1</sup>,  
and Sunil Pareek <sup>3</sup>

<sup>1</sup>Department of Food Science and Technology, National Institute of Food Technology Entrepreneurship and Management, Kundli, Sonipat 131028, Haryana, India

<sup>2</sup>Department of Food Technology, Harcourt Butler Technical University, Nawabganj, Kanpur 208002, Uttar Pradesh, India

<sup>3</sup>Department of Agriculture and Environmental Sciences, National Institute of Food Technology Entrepreneurship and Management, Kundli, Sonipat 131028, Haryana, India

Correspondence should be addressed to Anurag Singh; [anurag.niftem@gmail.com](mailto:anurag.niftem@gmail.com) and Sunil Pareek; [sunil\\_chiah@yahoo.co.in](mailto:sunil_chiah@yahoo.co.in)

Received 12 June 2022; Revised 18 September 2022; Accepted 8 October 2022; Published 7 November 2022

Academic Editor: Antonio Piga

Copyright © 2022 Meenatai Kamble et al. This is an open access article distributed under the Creative Commons Attribution License, which permits unrestricted use, distribution, and reproduction in any medium, provided the original work is properly cited.

Green banana (*Musa* spp.) is a significant source of starch (resistant starch ~50%), phenolics and flavonoid compounds, and minerals (K, Mg, Zn, and Fe). The utilization of green bananas in their fresh form is limited, whereas the drying of bananas provides the opportunity to use them for various purposes. Drying temperature and slice thickness are important to be optimized for drying of bananas as they affect the quality parameters. The present study was conducted using response surface methodology to optimize tray-drying temperatures (50–80°C) and slice thicknesses (2–8 mm) on the basis of phytochemical and physical parameters of dried green banana slices. The cubic model was found to be the best fit for most of the responses ( $R^2 = 0.95-1$ ), and the quadratic model was fit for water activity ( $a_w$ ) ( $R^2 = 0.92$ ). The optimized drying conditions were found as drying temperature of 50°C and slice thickness of 4.5 mm. Experimental responses exhibited maximum  $L^*$  (84.06),  $C^*$  (13.73), and  $h^o$  (83.53) and minimum losses of total phenolic content (89.22 mg GAE/100 g) and total flavonoid content (3.10 mg QE/100 g) along with lower  $a_w$  (0.25). The optimized green banana flour was rich in carbohydrates ( $77.25 \pm 0.06\%$ ) and low in fat ( $1.79 \pm 0.11\%$ ). The flour obtained had good flowability with a mean particle size of  $60.75 \pm 1.99 \mu\text{m}$ . Flour's gelatinization and decomposition temperatures were 102.7 and 292°C, respectively. In addition, flour's water absorption, oil absorption, and solubility were  $5.19 \pm 0.01$ ,  $1.58 \pm 0.01$ , and  $0.14 \pm 0.02$  g/g, respectively. Green bananas dried at optimized conditions resulted in a better product with less phytochemical loss than dried with other methods.

## 1. Introduction

The banana is the world's most perishable tropical fruit crop. It is cultivated in approximately 130 countries. It is the fourth most important staple crop after rice, wheat, and millet in terms of gross production value [1]. It is known as "poor man's fruit," eaten by millions of people, and has an essential impact on the economies of developing countries. Asia is the largest producer of bananas, contributing ~54% of global production, followed by America (26%), Africa

(17%), and Oceania (1.4%) [2]. India and China have been the world's largest banana producers, representing more than 40% of the world's total banana production [1].

Green banana is a significant source of carbohydrates (starch, resistant starch, and dietary fiber), antioxidants, vitamins (retinal (A), pyridoxine (B6), and ascorbic acid (C)), and minerals, especially potassium, sodium, and calcium [3]. The postharvest losses in green bananas are a significant issue influencing the production of bananas either quantitatively or qualitatively. Its climacteric nature

brings physiological changes after harvests, such as softening of the flesh, color change, and loss of weight. The improper handling, inappropriate cold storage, transportation, and postharvest bio-deterioration (microorganisms, insects, rodents, and birds) are responsible for bananas' ~30–50% postharvest losses [4–6]. Also, the temperature and humidity of storage or transport and cultivation are the main factors that cause green bananas' postharvest losses [4]. Therefore, postharvest losses can be managed by taking care of the harvest (using appropriate storage, cooling, packaging, and market system) and its processing (value addition or making perishable to nonperishable in nature). Nowadays, green banana flour is utilized as the functional ingredient in preparing gluten-free foods such as biscuits, pizza, bread, noodles, and spaghetti of low caloric value with partial or complete replacement of the wheat flour/maida [7]. It is the main ingredient of weaning food and soups.

Drying is a better approach to reduce postharvest losses by decreasing the banana moisture content and  $a_w$  resulting in declining rate of physical and biochemical reactions which are prone to microbial growth on the ripening of bananas. Phungamngoen et al. [8] reported that the *Salmonella anatum* contaminated cabbage tray drying at 50, 60, and 70°C showed a 3-log reduction of *Salmonella* within 1.8, 3.3, and 6 h dried at 50, 60, and 70°C, respectively. Convective tray drying is one of the most well-known drying strategies that are promptly accessible, simple to use, and has a lower initial installation cost than vacuum drying, freeze drying, and spray drying [9]; however, the main disadvantages of tray drying are the higher drying temperature, time, and energy consumption than the other advanced drying techniques [10].

Most researchers have studied the optimization of various drying techniques for ripe or semi-ripe banana slices, such as solar drying [11], tray drying [12], oven drying [13], vacuum drying [14], and microwave drying [15]. There is a paucity of literature on optimizing green banana tray-drying parameters too, with respect to the varying thickness. Reported studies have been conducted to optimize the drying parameters with respect to moisture content, drying rate, drying efficiency, moisture diffusivity, water adsorption, color, and thermal properties (specific heat, thermal conductivity, and thermal diffusivity) [16, 17]. The drying methods and conditions are product-specific, and the equal size of fruit slices is another essential prerequisite instead of whole fruit drying [18]. The whole process of fruit drying causes uneven drying, lower drying rate, and longer drying time, which negatively influence the appearance, phytochemicals, and nutritional value of dried fruit. Likewise, Kumar et al. [19] reported that the relatively decreased drying rates and longer drying times cause the degradation of natural pigments, nutrients, and morphological structure damage to food materials, constraining the utility of hot air dryers. Thus, drying a particular food with sample dimensions (thickness) must be optimized [18].

The lower/higher drying temperature and sample slice thickness other than the optimized conditions negatively influence the phytochemicals, color, nutritional content, and other physical characteristics of dried food, which

necessitate the optimization of tray drying. To the best of our knowledge, none of the existing studies have been considered for optimization based on the physical and phytochemical quality characteristics of dried green bananas. Therefore, the present study was conducted to determine the influence of a wide range of drying conditions and sample thickness on the quality of green banana flour using the response surface methodology (RSM). The criteria defined to assess the quality of tray-dried banana flour were color (lightness ( $L^*$ ), chroma ( $C^*$ ), and hue angle ( $h^\circ$ )), water activity ( $a_w$ ), total phenolic content (TPC), and total flavonoid content (TFC).

Fruits and vegetable powders rich in phytochemicals are generally analyzed for their TPC and TFC through spectrophotometric methods. Various flow properties of the food powders, namely, bulk density, tapped density, angle of repose, Carr index (CI) and Hausner ratio (HR), compressibility index, and particle size play a major role in industrial handling and application of food powders. Variation in these properties creates problems in the handling and storage of the powders. Similarly, thermal analysis and Fourier transform infrared spectrophotometer (FTIR) analysis of food powders are important to understand their thermal behavior and the presence of functional groups during processing. Proximate compositional analysis, total soluble solids (TSS), pH, titratable acidity (TA), water absorption capacity (WAC), solubility and, oil absorption capacity (OAC) are the important characteristics to understand the application of the food powder. Hence, in the present study, all these characteristics of the green banana powder developed were estimated.

## 2. Materials and Methods

**2.1. Raw Material and Sample Preparation.** The green cooking type banana fruit bunches with a totally green color were hand-harvested around the maturity of 110–120 days after flowering at Dinesh Farm, Manouli village, Sonipat, Haryana, India. The green banana bunches were washed with a 100 ppm sodium hypochlorite solution to disinfect and remove soil and dust matter adhered to the bunches as practiced by Kamble et al. [20]. Then, green banana bunches were separated into hands using the knife, hand-peeled, and mechanically sliced into different thicknesses using a slicer (Lavish Professional®, Sandeep Instrument and Chemicals, New Delhi, India). The banana slices were dried in a hot air tray dryer (Macro Scientific Works Pvt. Ltd., New Delhi, India) at varying temperatures as per the experimental design.

**2.2. Experimental Design for Optimization of Convective Tray-Drying Parameters.** RSM is the statistical tool generally used for optimization studies. Based on the preliminary experiments, the wide range of tray-drying temperatures (50–80°C) and banana slice thickness (2–8 mm) were selected as independent factors. Convective hot air-drying conditions affect the color values ( $L^*$ ,  $C^*$ ,  $h^\circ$ ) due to

TABLE 1: Experimental independent factors and levels used in tray drying of bananas.

Independent factors	Coded levels			
	-1	-0.33	0.33	1
A : temperature (°C)	50	60	70	80
B : thickness (mm)	2	4	6	8

enzymatic or nonenzymatic reactions. TFC and TPC are thermo-sensitive and are destroyed by thermal processing, and  $a_w$  is essential to predict the presence of unbound water responsible for the nonmicrobial and microbial reactions. Hence, the quality characteristics of dried banana slices were  $L^*$  value,  $C^*$  value,  $h^o$  value,  $a_w$ , TPC, and TFC were taken as response parameters. The experimental range and coded levels of the independent factors are given in Table 1.

Forty-eight experimental runs were suggested by Design-Expert 12.0, a statistical software package for two factors at four levels in triplicate (Table 2). All the response data from the proposed experiments were expressed in a generalized polynomial equation to generate a model, as shown in equation (1). The modeling, statistical analysis, and optimization were done with software support. The model output is shown in Table 3.

$$Y = \beta^o + \sum_{j=1}^k \beta_j X_j + \sum_{j=1}^k \beta_{jj} X_j^2 + \sum_i \sum_{<j=2}^k \beta_{ij} X_i X_j + \varepsilon, \quad (1)$$

where  $Y$  represents the predicted variable response,  $\beta^o$  is the constant of fitted response at the center point,  $\beta_j$ ,  $\beta_{ij}$ , and  $\beta_{jj}$  are coefficients of linear terms, interaction effects, and quadratic terms,  $\varepsilon$  is the random error, and  $X_i$  and  $X_j$  are independent variables, respectively.

The optimum convective tray-drying parameters were predicted by applying the constraints on variable responses in the RSM. Thus, the selected optimum drying condition resulted in the development of good-quality green banana slice flour.

**2.3. Flour Preparation.** The hot air tray-dried slices of different thicknesses were separately ground in a hammer mill (2 in 1, Classic Atta Chaki™, Rajkot, Gujarat, India) to obtain banana flour. The obtained flour was characterized for physicochemical characteristics to optimize the drying parameters.

#### 2.4. Determination of Response Parameters

**2.4.1. Color.** The digital colorimeter (Chroma-400, Konica Minolta, Japan) was used to determine the color values of green banana flour. It was precalibrated with black and white tiles before the measurement. The color parameters  $L^*$ ,  $a^*$ , and  $b^*$  were measured. The  $L^*$  value represents the brightness to blackness (0–100). The  $a^*$  value represents greenness ( $-a^*$ ) to redness ( $+a^*$ ). The  $b^*$  value refers to blueness ( $-b^*$ ) to yellowness ( $+b^*$ ). The hue ( $h^o$ ) measures the overall perception of the red, yellow, green, and blue color of the banana flour at an angle of  $0^\circ$ ,  $90^\circ$ ,  $180^\circ$ , and  $270^\circ$ .

The  $C^*$  measures its color in terms of purity, intensity, and saturation. The  $C^*$  and  $h^o$  values were calculated using

$$C^* = \sqrt{(a^*)^2 + (b^*)^2}, \quad (2)$$

$$h^o = \tan^{-1}\left(\frac{b^*}{a^*}\right). \quad (3)$$

**2.4.2. Water Activity ( $a_w$ ).** Banana flour's  $a_w$  was measured using the digital water activity meter (Aqua Lab, METER Group, Inc. USA) to estimate the unbound water vapor pressures, with an accuracy of  $\pm 0.003$ . It was precalibrated with milli-Q-water at  $25^\circ\text{C}$ .

#### 2.4.3. Estimation of Total Phenolic and Total Flavonoid Content

**(1) Sample Extraction.** The banana flour (1 g) was mixed with 25 mL of ethanol. The centrifuge tube containing the sample was placed in a shaker incubator (Biosan SIA, Environmental Shaker Incubator ES 20/60, Latvia) at  $37^\circ\text{C}$  with  $240 \times g$  shaking speed for 16 h to solubilize the phenolic and flavonoid compounds in ethanol during incubation. Then, it was centrifuged ( $3-18\text{KS}$ , Sigma Laborzeatrfugen GmbH, Germany) at  $6,000 \times g$  for 15 min, and the collected supernatant was added to a clean 50 mL falcon tube to estimate TPC and TFC.

**(2) Total Phenolic Content (TPC).** TPC was estimated using the Folin–Ciocalteu colorimetric method described by Padhi and Dwivedi [22] with slight modifications. The sample extract was added in 5 mL of Folin–Ciocalteu reagent and 4 mL sodium carbonate (7.5%), and it was mixed. The sample solution was incubated in a dark place at  $25^\circ\text{C}$  for 30 min. The amount of light absorbed by the sample was taken against the reagent blank at 760 nm on a UV-VIS spectrophotometer (Shimadzu, UV-1800, Japan) to determine the concentration of TPC in the sample. TPC was calculated from the gallic acid standard curve as per equation (4) (calibration equation:  $y = 6.0575x + 0.0033$ ;  $r^2 = 0.99$ ) and expressed as mg of gallic acid equivalents (GAE) in 100 g of green banana flour (dry weight basis).

$$\text{Total phenolic content} \left( \frac{\text{mgGAE}}{100\text{g}} \right) \quad (4)$$

$$= \frac{X \times \text{volume of extract}}{\text{weight of sample}} \times 100,$$

where  $X$  is the concentration of phenolic content (mg/mL).

**(3) Total Flavonoid Content (TFC).** The aluminum chloride colorimetric method was used to estimate the TFC as described by Padhi and Dwivedi [22] with slight modifications. The sample extract was added to 0.2 mL of 10% aluminum chloride ( $\text{AlCl}_3$ ) and mixed. After 2 min, 0.2 mL of 1 M potassium acetate and 5.6 mL of distilled water were added. The sample mixture was incubated in a dark environment at

TABLE 2: Experimental design for the tray-dried green banana slices and the response values.

Exp. no.	Temperature (°C)	Thickness (mm)	$L^*$	$C^*$	$h^o$	Water activity	Total phenolic content (mg/100 g of GAE)	Total flavonoid content (mg/100 g of QE)
1	50	2	84.12	14.23	82.57	0.25	108.65	3.33
2	50	2	84.2	14.48	83.14	0.25	109.68	3.23
3	50	2	84.6	14.32	83.10	0.25	108.37	3.30
4	60	2	84.33	13.21	83.00	0.24	52.20	3.07
5	60	2	84.03	14.14	81.78	0.25	53.16	2.98
6	60	2	84.65	13.97	82.10	0.25	53.44	3.08
7	70	2	80.47	12.74	81.20	0.24	48.99	2.89
8	70	2	80.68	13.75	81.22	0.24	49.13	3.03
9	80	2	71.4	12.73	78.72	0.23	32.08	2.10
10	80	2	72.42	12.67	78.39	0.23	31.48	2.10
11	80	2	71.4	12.57	78.53	0.23	33.51	1.99
12	80	2	71.4	12.61	78.52	0.23	32.27	2.09
13	50	4	84.7	13.69	82.78	0.25	92.83	3.09
14	50	4	84.7	14.02	83.57	0.25	92.82	3.15
15	50	4	83.31	13.92	83.65	0.25	90.96	3.17
16	60	4	83.47	12.41	82.27	0.24	38.99	2.84
17	60	4	83.54	12.71	82.36	0.24	40.00	2.82
18	60	4	83.38	12.90	82.70	0.24	40.92	2.79
19	70	4	81.91	12.01	81.96	0.24	39.85	2.70
20	70	4	80.97	11.87	80.74	0.24	40.12	2.65
21	70	4	81.47	11.76	81.29	0.24	40.20	2.68
22	70	4	81.65	11.67	82.37	0.24	40.20	2.66
23	80	4	73.72	11.73	78.35	0.23	24.93	2.00
24	80	4	73.69	11.70	79.16	0.23	24.93	1.93
25	80	4	73.95	11.90	78.80	0.23	24.93	1.95
26	50	6	84.39	13.81	83.47	0.25	79.28	2.98
27	50	6	84.52	13.81	83.51	0.24	79.41	2.93
28	60	6	83.68	12.41	82.87	0.25	31.66	2.56
29	60	6	83.81	12.20	81.66	0.24	32.11	2.56
30	60	6	84.29	12.22	82.33	0.24	32.11	2.56
31	70	6	81.41	11.78	81.51	0.23	32.90	2.52
32	70	6	82.35	11.60	81.07	0.24	31.77	2.50
33	70	6	81.43	11.81	81.48	0.24	32.87	2.52
34	70	6	81.41	11.78	81.51	0.23	32.90	2.52
35	70	6	82.35	11.60	81.07	0.24	31.77	2.53
36	70	6	81.43	11.81	81.48	0.24	32.87	2.52
37	80	6	74.47	11.49	78.86	0.23	20.58	1.88
38	50	8	83.9	13.57	83.91	0.25	77.69	2.54
39	50	8	84.41	13.16	83.80	0.24	75.90	2.64
40	50	8	84.97	13.18	83.77	0.25	76.88	2.56
41	60	8	83.84	12.04	82.70	0.25	32.85	2.07
42	60	8	83.92	12.06	82.71	0.25	31.64	2.07
43	60	8	84.19	12.13	82.90	0.24	32.17	2.05
44	70	8	82.19	11.68	81.58	0.24	35.34	2.07
45	80	8	74.62	11.42	79.71	0.23	24.67	1.71
46	80	8	74.33	11.35	78.88	0.23	24.42	1.64
47	80	8	74.4	11.13	79.29	0.23	24.61	1.54
48	80	8	74.55	11.06	79.53	0.23	24.55	1.68

25°C for 30 min. The UV-Vis spectrophotometer (Shimadzu, UV-1800, Japan) was used to read the amount of light absorbed by the sample against the reagent blank at 415 nm to estimate the concentration of TFC in the sample. The quercetin standard curve was prepared to calculate the TFC in mg of quercetin equivalent (QE) in 100 g of green banana flour (dry weight basis) using equation (5) (calibration equation:  $y = 0.3266x + 0.0005$ ;  $R^2 = 0.9986$ ).

$$\begin{aligned} \text{Total flavonoid content (TFC)} & \left( \frac{\text{mg QE}}{100\text{g}} \right) \\ & = \frac{X \times \text{volume of extract}}{\text{weight of sample}} \times 100, \end{aligned} \quad (5)$$

where, X is the concentration of flavonoid content (mg/mL).

TABLE 3: Model statistics and regression coefficient for each response of tray-drying condition.

Regression coefficient	$L^*$	$P$ value	$C^*$	$P$ value	$h^o$	$P$ value	Water activity	$P$ value	Total phenolic content (mg/100 g GAE)	$P$ value	Total flavonoid content (mg/100 g QE)	$P$ value
Intercept	83.27		12.11		82.02		0.24		33.00		2.67	
A	-3.18*	<0.0001	-1.07*	<0.0001	-1.40*	<0.0001	-0.01*	<0.0001	4.40*	<0.0001	-0.06	0.0615
B	0.24	0.4360	-0.40*	0.0230	-0.28	0.2807	0.00*	0.02	-12.15*	<0.0001	-0.32*	<0.0001
AB	0.69*	<0.0001	-0.08	0.1919	-0.03	0.7776	0.00	0.5724	5.98*	<0.0001	0.07*	<0.0001
$A^2$	-4.17*	<0.0001	0.47*	<0.0001	-0.93*	<0.0001	0.00*	<0.0001	20.43*	<0.0001	-0.17*	<0.0001
$B^2$	-0.26	0.0900	0.38*	<0.0001	0.08	0.5479	0.00	0.0787	7.21*	<0.0001	-0.12*	<0.0001
$A^2B$	0.55*	0.0094	0.25*	0.0332	0.25	0.1419	—	—	-1.57*	<0.0001	0.20*	<0.0001
$AB^2$	-0.74*	0.0008	0.18	0.1152	0.05	0.7704	—	—	-0.72*	0.0284	0.03	0.1161
$A^3$	-1.78*	<0.0001	-0.06	0.7398	-0.89*	0.0024	—	—	-35.89*	<0.0001	-0.51*	<0.0001
$B^3$	-0.08	0.8132	-0.47*	0.0128	0.47	0.0921	—	—	3.79*	<0.0001	-0.16*	<0.0001
Lack of fit	2.35	0.0542	2.01	0.0940	0.16	0.9842	1.41	0.22	2.33	0.0562	0.93	0.48
F-value	554.27*	<0.0001	81.50*	<0.0001	112.74*	<0.0001	92.37*	<0.0001	7224.00*	<0.0001	614.45*	<0.0001
$R^2$ value	0.99	—	0.95	—	0.96	—	0.92	—	1.00	—	0.99	—
CV (%)	0.54	—	1.91	—	0.45	—	0.91	—	1.45	—	1.77	—
Standard deviation	0.44	—	0.24	—	0.36	—	0.00	—	0.69	—	0.04	—

## 2.5. Physicochemical Characterization of Optimized Green Banana Flour

**2.5.1. Proximate Compositional Analysis.** The proximate analysis of banana flour was determined according to the methodology described in AOAC [23]. The moisture content was analyzed via desiccating sample moisture in a hot air oven at 105°C to achieve the constant sample weight repeatedly three consequent times. The fat content was

estimated by the extraction of petroleum ether using the Soxhlet apparatus. The defatted sample was used to estimate crude fiber using acid-alkali hydrolysis (1.25% of sodium hydroxide and 1.25% of sulfuric acid). The crude protein was estimated using the Kjeldahl method, and the conversion factor used for protein estimation was nitrogen%  $\times$  6.25. The total carbohydrate percentage was calculated using [24]

$$\text{Total carbohydrate (\%)} = 100 - [\text{moisture (\%)} + \text{fat (\%)} + \text{protein (\%)} + \text{crude fiber (\%)} + \text{ash (\%)}]. \quad (6)$$

**2.5.2. Total Soluble Solid (TSS).** The TSS of the banana flour was estimated as per the method suggested by Rayo et al. [25]. The flour was dissolved in distilled water at a ratio of 1 : 10 w/v. The digital refractometer (RX-7000i, Atago Co., Ltd., Japan) was used to estimate the TSS content of banana flour. Before taking the measurements, the refractometer was calibrated with distilled water at 20°C. The test supernatant was kept on the refractometer prism, and the TSS was expressed in %.

**2.5.3. pH.** The digital pH meter (pH Tutor, Euteck Instruments, Cyber Scan, India) was used to measure the hydrogen ion activity of the flour (acidity or alkalinity) at  $25 \pm 2^\circ\text{C}$ . The pH meter was calibrated with buffers of pH 4, 7, and 9.2 before the measurement.

**2.5.4. Titratable Acidity (TA).** The alkali titration method was used to estimate TA in terms of citric acid as practiced by Padhi and Dwivedi [22]. The aliquots were titrated with 0.1 N sodium hydroxide (NaOH) solution after adding 1-2 drops of phenolphthalein as a color indicator. The titrated solution turned pink in color at the endpoint of the titration, and a burette reading was noted. TA was calculated as given in

$$\text{Titrateable acidity (TA) (\%)} = \frac{x \times 0.1 \text{ N NaOH} \times \text{equivalent weight of citric acid}}{\text{weight of sample} \times \text{aliquot taken} \times 1000} \times 100, \quad (7)$$

where,  $x$  is the titer value.

## 2.6. Functional Properties of Green Banana Flour

### 2.6.1. Water Absorption Capacity (WAC) and Solubility.

The WAC measures the ability of banana flour to absorb water, which was determined according to the procedure reported by Taiwo and Babalola [27] with slight modifications. The banana flour was dispersed in distilled water at a ratio of 1 : 10. It was mixed and centrifuged (3–18KS, Sigma Laborzeatrfugen GmbH, Germany) at  $4,000 \times g$  for 20 min. The supernatant was decanted carefully by keeping the tube at an angle of  $45^\circ$  for 10 min. The supernatant was desiccated, and the residual solid content was weighed to calculate the solubility of banana flour using equation (9). The solubility was measured as the ability of flour to form the homogeneous solution with water and was expressed in gram soluble solids per gram of flour. Also, the banana flour containing absorbed water was weighed to see the WAC and expressed as a gram increase in sample weight per gram of flour.

$$\text{Water absorption capacity (WAC)} \left( \frac{\text{g}}{\text{g}} \right) = \frac{W_2 - W_1}{W_1}, \quad (8)$$

$$\text{Solubility} \left( \frac{\text{g}}{\text{g}} \right) = \frac{W_3}{W_1}, \quad (9)$$

where  $W_1$ ,  $W_2$ , and  $W_3$  are the weight of the sample, the weight of the sample absorbed by water after centrifugation, and the weight of soluble solids in the supernatant after evaporation, respectively.

**2.6.2. Oil Absorption Capacity (OAC).** The OAC measures the ability of any flour to absorb the oil, which was estimated according to the procedure reported by Taiwo and Babalola [27]. The banana flour was dispersed in the soybean oil at a ratio of 1 : 10 in a 50 mL Falcon centrifuge tube. It was mixed and centrifuged (3–18KS, Sigma Laborzeatrfugen GmbH, Germany) at  $4,000 \times g$  for 20 min. The nonabsorbed oil was decanted carefully by keeping the falcon tube at an angle of  $45^\circ$  for 10 min. Then, the oil absorbed by the sample was weighed. The OAC of flour was estimated by using

$$\text{Oil absorption capacity (OAC)} \left( \frac{\text{g}}{\text{g}} \right) = \frac{W_2 - W_1}{W_1}, \quad (10)$$

where,  $W_1$ ,  $W_2$  and are the weight of the sample, the weight of the sample absorbed by oil after centrifugation, respectively.

## 2.7. Flow Properties of Banana Flour

**2.7.1. Bulk Density.** The bulk density was determined as per the method described by Taiwo and Babalola [27]. The bulk density was measured as the ratio of the mass of porous flour to the volume of porous flour. The banana flour (5 g) was filled in 25 mL of a graduated measuring cylinder. Then, the

volume occupied by the flour was noted. The bulk density of flour was expressed in  $\text{g}/\text{cm}^3$  and calculated using

$$\text{Bulk density } (\rho_b) \left( \frac{\text{g}}{\text{cm}^3} \right) = \frac{\text{mass of banana flour}}{\text{volume of banana flour}}, \quad (11)$$

**2.7.2. Tapped Density.** Tapped density was determined as per the method described by Taiwo and Babalola [27]. The banana flour (5 g) was filled into a 25 mL of graduated measuring cylinder and tapped manually on a rubber mat up to 25 times. The volume of banana flour was noted, and the tapped density of banana flour was calculated using equation (12). The tapped density of flour was expressed in  $\text{g}/\text{cm}^3$ .

$$\begin{aligned} \text{Tapped density } (\rho_t) \left( \frac{\text{g}}{\text{cm}^3} \right) \\ = \frac{\text{Mass of banana flour}}{\text{Volume of compact banana flour}}. \end{aligned} \quad (12)$$

**2.7.3. Angle of Repose.** It is necessary to assess the flowability of granular materials. Also, it is mainly used in the design of industrial equipment such as hoppers, silos, and belt conveyors. The angle of repose was estimated as per the method suggested by Anuar et al. [28]. The sample (50 g) was weighed and passed through the funnel. The angle of repose of flour at  $25-30^\circ$  means excellent flowability,  $31-35^\circ$  means good flowability of flour,  $36-40^\circ$  means fair flowability of flour, and  $41-45^\circ$  and  $45-55^\circ$  mean passable and poor flowability of the flour. The maximum possible angle formed between the surface of the heap of flour and the flat surface was calculated using

$$\text{Angle of repose } (\alpha) = \tan^{-1} \left( \frac{2h}{r} \right), \quad (13)$$

where  $h$  is the height of the flour heap (cm) and  $r$  is the radius of the flour heap (cm).

**2.7.4. Carr Index (CI) and Hausner Ratio (HR).** CI and HR characterize the flowability and cohesiveness of flour. It was determined using the tapped density and bulk density. According to Turchiuli et al. [29], HR of the flour was classified as  $\text{HR} < 1.2$  means free-flowing,  $1.2 < \text{HR} < 1.4$  means intermediate free-flowing, and  $\text{HR} > 1.4$  means very cohesive. The flowability of flour is classified according to Rayo et al. [25] as very good flowability if  $\text{CI} < 15$ , good if CI is 15–20, fair if CI is 20–35, and poorly flowable if CI is 35–45. The HR and CI were estimated using

$$\text{HR} = \frac{\rho_t}{\rho_b}, \quad (14)$$

$$\text{CI} = \frac{\rho_t - \rho_b}{\rho_t} \times 100, \quad (15)$$

where,  $\rho_t$  is the tapped density of flour ( $\text{g}/\text{m}^3$ ) and  $\rho_b$  ( $\text{g}/\text{m}^3$ ), and  $\rho_b$  is the bulk density of flour ( $\text{g}/\text{m}^3$ ).

**2.7.5. Compressibility Index.** The compressibility index is used to know the capability of flour to be compacted. According to Mirhosseini and Amid [30], the compressibility index of flour was classified as <10 means very good, 11–15 means good, 16–20 means fair, 21–25 means passable, 26–31 means poor, and 32–37 means very poor. It was calculated using the porous and compacted green banana flour volume as represented in

$$\text{Compressibility index} = \frac{V_p - V_c}{V_p} \times 100, \quad (16)$$

where,  $V_p$  is the volume of porous flour ( $\text{m}^3$ ) and  $V_c$  is the volume of compact flour ( $\text{m}^3$ )

**2.8. Particle Size Analysis.** The dry laser diffraction particle size analyzer (PSA 1090 LD, Anton Paar, Austria) was used to determine the particle size of flour as suggested by Ahmed et al. [31]. The refractive index of water (1.32) and green banana flour (1.52) was used as the reference for measurement. The particle size distribution analysis based on 10, 50, and 90% of particle proportions was designed as D10, D50, and D90. Also, the mean particle size  $D$  and the span value of flour were determined.

**2.9. Thermal Analysis.** The differential scanning calorimetry (DSC) (200F3, Maia, NETZSCH, Germany), thermogravimetric analysis (TGA), and differential thermogravimetric (DTGA) (NETZSCH TG 209F1 Libra TGA209F1D-0072, Germany) were done to estimate the phase transition, simultaneous change in sample mass, and heat flow with respect to the change in temperature, respectively. For DSC, 2 mg of banana flour and 7  $\mu\text{L}$  of distilled water were taken in an aluminum pan, mixed, and covered with a lid. The sealed sample pan was equilibrated for 60 min at room temperature. Then it was scanned at 30 to 250°C in DSC. For TGA and DTGA, 5 mg flour was taken in the alumina ceramic crucible and kept in the sample holder. The TGA was run at 30 to 800°C. The heating rate was constant (10°C/min) for the DSC and TGA with a continuous supply of nitrogen at 20 mL/min. Proteusnetzsch software (version 6.1.10) was used to carry out the data analysis.

**2.10. Fourier Transform Infrared Spectrophotometer (FTIR) Analysis.** The presence of various bonds associated with a functional group in flour was investigated using FTIR (Carey 630, Agilent, USA). The banana flour was placed on an attenuated total reflection plate and scanned for spectra in the range of 4,000–400  $\text{cm}^{-1}$ . The entire attenuated reflection plate was cleaned before analysis by using isopropanol. The sample spectra were measured against the background spectrum. The sampling noise was removed by smoothing, and all measured peaks were denoted by peaking functions to know the absorption spectrum of the functional group.

**2.11. Statistical Analysis.** The optimization, data analysis, and response surface plots were created using Design-Expert 12.0 software (Stat-Ease Inc., Minneapolis, USA). The accuracy and fit statistics of the model were studied based on analysis of variance (ANOVA) with a significant ( $p < 0.05$ ) model F-value and nonsignificant lack of fit ( $p > 0.05$ ), the highest coefficient of determination ( $R^2$ ), minimum coefficient of variation, and standard deviation. The regression coefficient of model responses enabled us to predict the interactive effect of different variables on dried banana flour quality parameters. The model's efficiency was validated by performing the proposed preliminaries and comparing their output with the predicted results. The IBM SPSS program, version 26 (SPSS Inc., Chicago, Illinois, USA), was used for descriptive statistical analysis, and results were expressed as mean values  $\pm$  standard deviation (SD).

### 3. Results and Discussion

#### 3.1. Influence of Tray-Drying Parameters on Responses and Model Fitting

**3.1.1. Lightness ( $L^*$ ), Chroma ( $C^*$ ), and Hue Angle ( $h^\circ$ ).** The color of dried green banana slice flour is an essential parameter concerning consumer preference and the quality of a final product. The color of the tray-dried sample was evaluated based on  $L^*$ ,  $C^*$ , and  $h^\circ$ . The overall experimental  $L^*$ ,  $C^*$ , and  $h^\circ$  values of tray-dried green banana flour varied from 71.4–84.97, 11.06–14.48, and 78.34–83.91, respectively (Table 2). The  $L^*$ ,  $C^*$ , and  $h^\circ$  values representing the lightness, color intensity, and saturation, and color characterization of flour (shift from red to cream-yellow color), were improved by reducing the drying temperature from 80 to 50°C and the sample thickness (8–2 mm) (Table 2, Figure 1). The polynomial equation was used to model experimental  $L^*$ ,  $C^*$ , and  $h^\circ$  values to predict the influence of drying parameters (independent factors) on the color value of flour. The analysis of variance of the  $L^*$ ,  $C^*$ , and  $h^\circ$  models indicate that the cubic model was significant ( $p < 0.05$ ) with F-values of 554.27, 81.50, and 112.74 (Equations (17)–(19)). Also, the nonsignificant lack of fit ( $p > 0.05$ ) F values were 2.35, 2.01, and 0.16, relative to pure error, showing good model predictability (Table 3). The interaction effect between experimental independent factors on  $L^*$ ,  $C^*$ , and  $h^\circ$  value of tray-dried flour showed a three-dimensional response surface plot (Figures 1(a)–1(c)). The significant ( $p < 0.05$ ) negative reduction of  $L^*$  and  $h^\circ$  values were observed with an increase in drying temperature, and the  $C^*$  value was negatively ( $p < 0.05$ ) influenced by the increase in drying temperature and slice thickness. The significant ( $p < 0.05$ ) influence of linear (A and B), interaction (AB,  $A^2B$ , and  $AB^2$ ), quadratic ( $A^2$  and  $B^2$ ), and cubic effect of drying temperature and thicknesses ( $A^3$  and  $B^3$ ), on  $L^*$ ,  $C^*$ , and  $h^\circ$  models were predicted through the regression coefficient of  $L^*$ ,  $C^*$ , and  $h^\circ$  models (Table 3). This significant variation in the  $L^*$ ,  $C^*$ , and  $h^\circ$  values of banana flour might be due to the nonenzymatic and enzymatic reactions of polyphenols with the oxygen and polyphenol oxidase enzyme resulting from an increase in tray-drying temperature and sample thickness

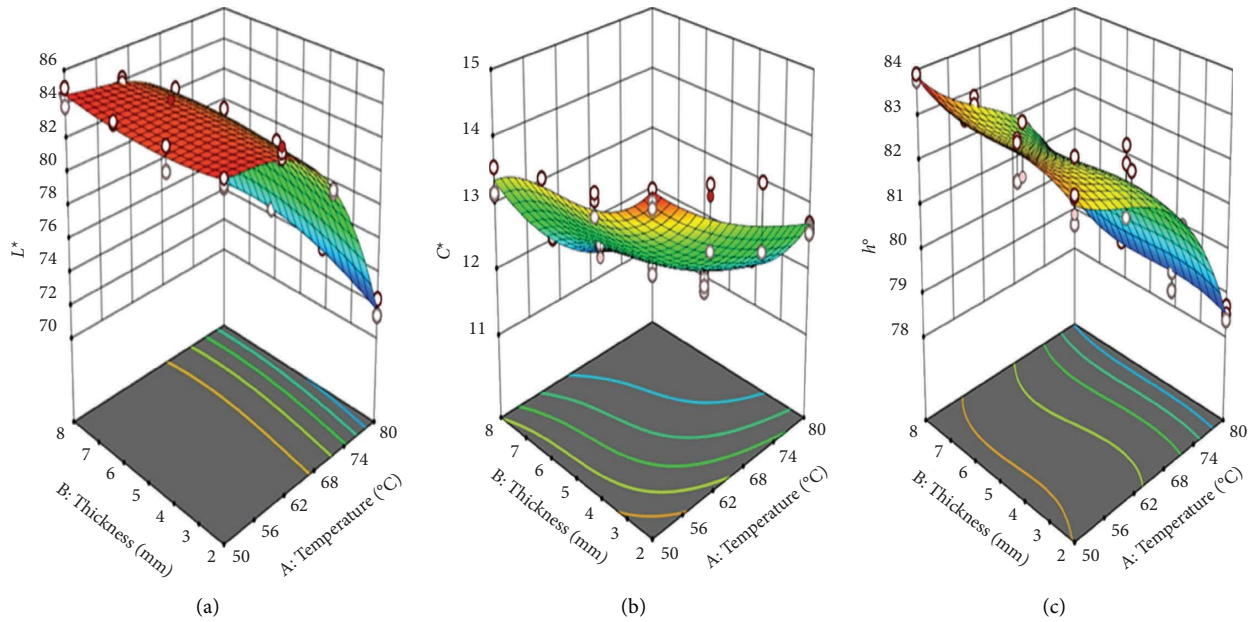


FIGURE 1: Influence of tray-drying conditions on (a)  $L^*$ , (b)  $C^*$ , and (c)  $h^{\circ}$  value of green banana flour.

(independent factors). Several studies showed that various factors negatively influence the color characteristic of the dried product, such as different drying temperatures, drying methods, rate of airflow, drying time, slice thickness, poor stability of pigmented compounds or thermal degradation, oxidative reactions, Maillard reactions, and caramelization of carbohydrates [12, 32–36]. A light yellowish color is mainly associated with green banana polyphenolic, flavonoid, lutein,  $\alpha$ -carotene, and  $\beta$ -carotene compounds [37]. The phenolic compounds in green bananas react with the oxygen and polyphenol oxidase enzyme, causing enzymatic browning reactions [38]. Similarly, Junqueira et al. [39] described that the nonenzymatic or enzymatic browning reaction could occur after cells collapse during the drying.

Various studies reported by the researchers found that the significant reduction in  $L^*$  and  $h^{\circ}$  value of oven-dried

‘Luvhele’ and ‘Mabonde’ bananas might be due to the oxidative reaction and degradation of pigmented compounds increased with an increase in the drying temperature (40–60°C) [13]. Likewise, Thuwapanichayanan et al. [12] reported a nonsignificant reduction in dried banana slices’  $L^*$  and  $h^{\circ}$  values with an increased tray-drying temperature of 70–100°C. Also, Kohli et al. [35] reported that the different drying temperatures (40–70°C) significantly influenced the  $h^{\circ}$  and  $C^*$  values of dried asparagus roots. Furthermore, the convectively tray-dried spine gourd (*Momordica dioica*) slices (2.5–3 mm thick) dried at 40–70°C presented a significant ( $p < 0.05$ ) difference in the  $L^*$  value ranging from  $78.55 \pm 0.66$  to  $83.74 \pm 0.14$  [19]. In the same way, the drying temperature of (45–75°C) and sweet potato slice thicknesses (2–6 mm) had a significant ( $p < 0.05$ ) effect on the  $L^*$ ,  $C^*$ , and  $h^{\circ}$  values of tray-dried sweet potatoes [34].

$$L^* = 83.27 - 3.18^*A_1 + 0.24^*B_2 - 4.17^*A_1^2 - 0.26^*B_2^2 + 0.69^*A_1B_2 + 0.55^*A_1^2B_2 - 0.74^*A_1B_2^2 - 1.78^*A_1^3 - 0.08^*B_2^3; (R^2 = 0.99), \quad (17)$$

$$C^* = 12.11 - 1.07^*A_1 - 0.40^*B_2 + 0.47^*$$

$$A_1^2 + 0.38^*B_2^2 - 0.08^*A_1B_2 + 0.25^*A_1^2B_2 + 0.18^*A_1B_2^2 - 0.06^*A_1^3 - 0.47^*B_2^3; (R^2 = 0.95), \quad (18)$$

$$h^{\circ} = 82.02 - 1.40^*A_1 - 0.28^*B_2 - 0.93^*A_1^2 + 0.08^*B_2^2 - 0.03^*A_1B_2 + 0.25^*A_1^2B_2 + 0.045^*A_1B_2^2 - 0.89^*A_1^3 + 0.467^*B_2^3; (R^2 = 0.96). \quad (19)$$

**3.1.2. Water Activity ( $a_w$ ).** The  $a_w$  is an essential parameter in arresting the nonmicrobial reactions and microbial growth. Lowering the  $a_w$  of food by drying is used in food preservation and development of different types of shelf-stable foods. The  $a_w$  of tray-dried green banana flour was found between 0.227 and 0.252. The interaction effect between independent factors on tray-dried green banana flour's  $a_w$  showed a three-dimensional response surface plot for the quality characterization of banana flour (Figure 2). The significant ( $p < 0.05$ ) positive effect on the linear decrease in  $a_w$  of tray-dried banana flour with increased drying temperature triggers removal of unbound water (free water molecules). The experimental results of the  $a_w$  were used in a polynomial equation to obtain the water activity ( $a_w$ ) model to interpret how the tray-drying parameters affect the  $a_w$

$$\text{Water activity } (a_w) = 0.24 - 0.01 * A_1 - 0.00 * B_2 - 0.0036 * A_1^2 + 0.0013 * B_2^2 - 0.00 * A_1 B_2; (R^2 = 0.92). \quad (20)$$

**3.1.3. Total Phenolic Content.** The phenolic compounds of bananas have antioxidant activity and are decreased due to thermal processing. TPC of tray-dried green banana flour ranged from 20.58 to 109.68 mg GAE/100 g. The influence of a wide range of tray-drying temperatures and sample thickness on the TPC of banana flour was better predicted by modeling the experimental results of TPC as a polynomial equation. The cubic model best fits the experimental data, and their analysis of variance showed the model is highly significant ( $p > 0.05$ ) with an F-value of 7224. The F-value of lack of fit was 2.33 ( $p > 0.05$ ), showing the model's excellent predictability. The coefficient of determination of the model ( $R^2$  0.99), the coefficient of variance (1.45%), and standard deviation (0.68) values were obtained, suggesting that this model is fit (Equation 21). The interaction effect of tray-drying temperatures and sample thickness on the TPC of flour showed the three-dimensional response surface plot (Figure 3). The main effect of tray-drying temperature and sample thickness ( $A$  and  $B$ ) and its interaction ( $AB$ ,  $A^2B$ , and  $AB^2$ ), quadratic ( $A^2$  and  $B^2$ ), and cubic effects ( $A^3$  and  $B^3$ ), had a significant impact on the TPC of tray-dried

$$\begin{aligned} \text{Total phenolic content} = & 33 + 4.40 * A_1 - 12.15 * B_2 + 20.43 * A_1^2 + 7.21 * B_2^2 + 5.98 * A_1 B_2 \\ & - 1.57 * A_1^2 B_2 - 0.72 * A_1 B_2^2 - 35.89 * A_1^3 + 3.79 * B_2^3; (R^2 = 1). \end{aligned} \quad (21)$$

**3.1.4. Total Flavonoid Content (TFC).** The flavonoids are part of naturally occurring phenolic compounds which are sensitive to thermal processing, and their losses are mostly found on convective hot air drying [34, 43]. The TFC of tray-dried green banana flour was found in a range of

of banana flour (Equation 20). The analysis of variance showed that the  $a_w$  was better predicted in the quadratic model, with a significant ( $p < 0.05$ ) F-value of 92.37 (Table 3). The model fit in terms of coefficient of determination value was closer to 1, and the lower coefficient of variance and deviation value showed the  $a_w$  model is suitable (Table 3, Equation 20). The main effect of tray-drying temperature and sample thickness ( $A$  and  $B$ ) and the quadratic effect of tray-drying temperature ( $A^2$ ) significantly ( $p < 0.05$ ) affected the  $a_w$  of banana flour (Table 3). In the same way, Savas [34] reported that the convective drying of sweet potato slices at different temperatures (45–75°C) and sweet potato slice thicknesses (2–6 mm) showed a positive reduction in the  $a_w$  with an increase in drying temperature and a decrease in sample thickness.

banana flour (Table 3). Although the banana is rich in phenolics, the increase in tray-drying temperature (50–80°C) and sample thickness (2–8 mm) had a negative effect on TPC. This decrease in TPC of banana flour might be due to the degradation of temperature-sensitive phenolic components by convective tray drying. Some of the TPC and TFC components are highly sensitive to convective drying, and loss in TPC content can be minimized by optimization.

A study reported that a significant reduction in TPC might be due to drying temperature and binding of phenolic components with other components like protein, resulting in structural changes in phenol [19]. Erbay and Icier [40] reported that convective drying of olive leaves at 40–60°C with air velocity of 0.5–1.5 m/s and process time 240–480 min increases the losses of percent TPC of olive leaves (8.13–37.25%) with the increase in drying temperature, process time, and air velocity. Similarly, Onal et al. [41] reported that the drying temperature releases the bound phenolic compounds and their derivatives, causing the partial breakdown of lignin and phenolic compounds. Correspondingly, elephant foot yam was tray dried at 40–70°C and showed variation in the TPC (0.01–0.005 mg/100 g) [42].

1.53–3.33 mg QE/100 g (Table 3, Figure 4). These losses in the flavonoid content of banana flour can be minimized by optimization. The effect of independent factors on the TFC of flour was interpreted by fitting the experimental result in the polynomial equation. The model fitting of TFC was better interpreted in the cubic model with a significant value of 614.45 (Table 3, Equation 22). The fit statistic of the model was predicted in terms of the highest  $R^2$  value and lowest

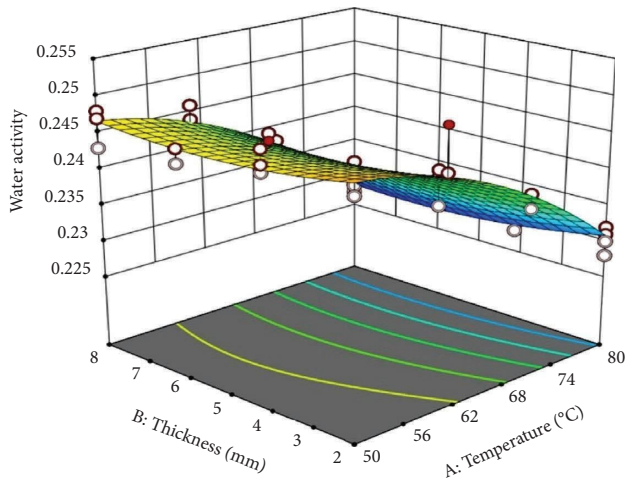


FIGURE 2: Influence of tray-drying conditions on water activity ( $a_w$ ) of banana flour.

coefficient of variance and standard deviation (Table 3). The interaction effect of independent factors on the TFC is represented in the three-dimensional response surface plot (Figure 4). The regression coefficient of the cubic model represents the expected change in TFC per unit change in independent factor (drying temperature and sample thickness), and all remaining factors are held constant. The linear effect of sample thickness (B) and interaction (AB and A2B), squared ( $A^2$  &  $B^2$ ), and cubic ( $A^3$  and  $B^3$ ) effects of drying temperature and thickness were identified as a significant ( $P < 0.05$ ) decrease in the TFC. The lower drying temperature and maximum thickness of the banana slice required the maximum drying time resulting in more degradation of TFC. The lower drying temperature and moderate banana slice thickness observed the minimum loss of TFC (Figure 4). Rababah et al. [43] reported that the convective hot air drying of fresh mint, sage, thyme, and lemon balm at 40°C showed a significant decrease in TFC of 298.5–90.6, 273.5–101.3, 260.3–104.7, and 252.9–97.8 mg of catechin equivalent/100 g, respectively. Jha and Sit [44] observed a significant increase in the TFC degradation rate of *T. chebula* fruit with an increase in temperature from 60 to 80°C, and degradation of TFC follows the first order kinetic. In the

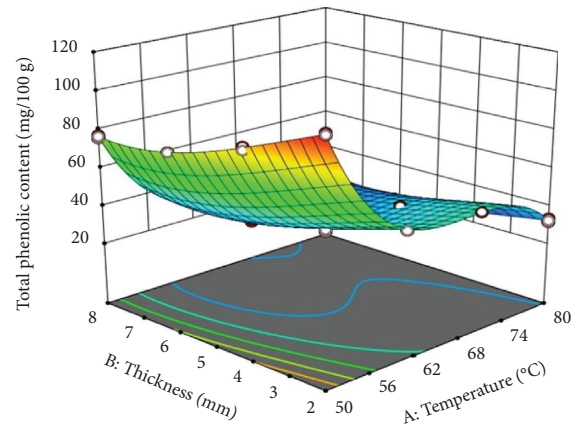


FIGURE 3: Influence of tray-drying conditions on the total phenolic content of green banana flour.

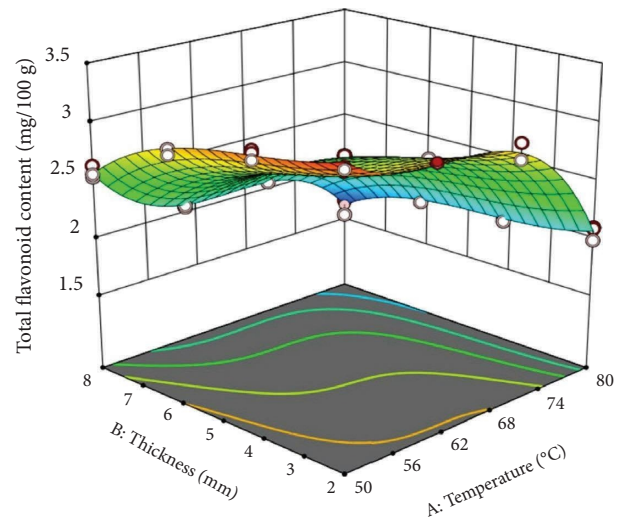


FIGURE 4: Influence of tray-drying condition on the total flavonoid content of green banana flour.

same way, the elephant foot yam was hot air tray dried at 40–70°C, and the difference in TFC ranges from (1.4–0.97 mg/100 g) [42].

$$\begin{aligned} \text{Total flavonoid content} = & 2.67 - 0.06 * A_1 - 0.32 * B_2 - 0.17 * A_1^2 - 0.12 * B_2^2 + 0.07 * A_1 B_2 \\ & + 0.20 * A_1^2 B_2 + 0.03 * A_1 B_2^2 - 0.51 * A_1^3 - 0.16 * B_2^3; (R^2 = 0.99). \end{aligned} \quad (22)$$

**3.2. Optimization and Validation of Drying Condition.** Green bananas' tray-drying process parameters were optimized based on fixed-set goals. Design-Expert software generated the possible solution for independent factors and their corresponding responses. The model was validated by performing triplicate experiments generated from Design-

Expert software and compared with the experimental value (Table 4). Green banana's ideal convective tray-drying process parameters were viewed as tray-drying temperature of 50°C and slice thickness of 4.29 mm. The predicted slice thickness of 4.29 mm was difficult to set in the automatic slicer. Therefore, the sample slice thickness of 4.5 mm and drying temperature of 50°C were considered ideal process parameters to validate the experiment. The experimental responses were obtained as  $L^*$  84.06,  $C^*$  13.73,  $h^*$  83.53, TPC

TABLE 4: Validation of predicted results at optimum tray-drying condition.

Response parameters	Predicted values	Experimental values	Error (%)
$L^*$	84.07	$84.06 \pm 0.16$	-0.01
$C^*$	13.75	$13.73 \pm 0.13$	-0.16
$h^\circ$	83.37	$83.53 \pm 0.23$	0.19
Water activity ( $a_w$ )	0.25	$0.25 \pm 0.00$	0.54
Total phenolic content (mg GAE/100 g)	89.98	$89.22 \pm 0.99$	-0.85
Total flavonoid content (mg quercetin/100 g)	3.12	$3.10 \pm 0.01$	-0.41

89.22 mg GAE/100 g, TFC 3.10 mg QE/100 g, and  $a_w$  0.25, respectively (Table 4). The responses obtained at an optimized condition showed minimum changes/losses in variables. The experimental values were near the predicted values showing that the optimized conditions (at 50°C with slice thickness of 4.5 mm) suggested by the software are acceptable. The parameters of experimental response were condition dependent. They are affected by drying temperature and time, air velocity, sample thickness, and varietal difference. Because of this, experimental values of optimized banana flour showing the variation over the previously reported findings from non-optimized processing condition are represented in Table 4. Thuwapanichayanan et al. [12], who had dried the banana slices (3 mm) at 70–100°C, reported the maximum  $h^\circ$  of 79.35° at 70°C compared to those dried at 90 ( $h^\circ$  78.59°) and 100°C ( $h^\circ$  73.16°). Olusegun-Omolola et al. [13] reported that the significant difference in  $h^\circ$  values of banana flour (74.60 and 68.99°) obtained at 47.56 and 68.99°C might be due to the oxidation and degradation of overall color with a rise in drying temperature. The obtained findings of water activity agreed with Savas [34] who reported the lowest  $a_w$  of 0.36 of dried sweet potato slice at an optimized drying condition of 75°C for 4.42 h with a sample slice thickness of 6 mm. Fatemeh et al. [45] reported that slices of both varieties of green cavendish banana and green dream banana dried under the same condition (50°C with slice thickness of 2 mm). The total phenolic content (373.88 mg GAE/100 g) and flavonoid content (281.18 catechin mg/100 g) in green cavendish banana flour was found to be higher than those of green banana flour (94.25 mg GAE/100 g and 82.64 mg catechin/100 g).

### 3.3. Characterization of Optimized Convective Tray-Dried Green Banana Flour

**3.3.1. Proximate Composition.** The proximate composition of green banana flour obtained at optimized drying conditions is given in Table 5. The results revealed that the moisture content of green banana flour was  $9.99 \pm 0.04\%$ . The fat, protein, total carbohydrate, ash, crude fiber, TA (as citric acid), pH, and TSS of flour were  $1.79 \pm 0.11\%$ ,  $1.23 \pm 0.04\%$ ,  $77.25 \pm 0.06\%$ ,  $5.10 \pm 0.04\%$ ,  $4.66 \pm 0.04\%$ ,  $0.55 \pm 0.03\%$ ,  $6.01 \pm 0.00$ , and  $0.72 \pm 0.00\%$ , respectively (Table 5). Kumar et al. [46] reported that the physicochemical composition of hot air-forced convectively dried five different varieties of green bananas namely, “Grand Naine”, “Monthan”, “Saba”, “Nendran”, and “Popoulu” slices (4 mm), obtained at 55°C showed the fat contents, protein content, and TA were in the ranges of  $0.17 \pm 0.01$ – $0.61 \pm 0.20\%$ ,  $3.53 \pm 0.41$

– $4.89 \pm 0.21\%$ , and  $0.61 \pm 0.03$ – $0.85 \pm 0.02\%$ . The commercial banana flour manufactured by Kunachia LLC, Davie, FL, USA, had a pH of 5.07 [47]. Our findings varied with the reported composition of green banana flour. It might be due to the varietal differences, maturity stage, drying method, drying temperature, airflow rate, and fruit dimension of green bananas.

**3.3.2. Functional Properties.** The WAC, OAC, and solubility of green banana flour were obtained as  $5.19 \pm 0.01$ ,  $1.58 \pm 0.01$ , and  $0.14 \pm 0.02$  g/g, respectively (Table 5). The results were not in agreement with those of Huang et al. [47], who reported WAC (3.08 g/g) and OAC (0.94 g/g) of commercial green banana flour manufactured by Kunachia LLC, Davie, FL, USA. It might be due to variations in the starch content in the fruit. The starch contains more hydrophilic sites that enable more water absorption because of interaction with the hydrogen bond of water molecules. Banana flour’s functional properties generally depend on its composition (resistant starch, amylose content, dietary fiber, and protein) and the interaction condition of oil/water [46]. Also, these properties depend on the particle size of flour, morphology, and flow properties (porosity and density). They are useful in new product formulation, mainly in bakery and fortified foods like baby food and snacks.

**3.3.3. Particle Size Distribution and Flow Properties.** The cumulative distribution curve represents the volume content of particle size as D10, D50, and D90. Ten percent of banana flour was less than  $11.45 \pm 0.17 \mu\text{m}$ , 50% of banana flour was  $<49.70 \pm 2.01 \mu\text{m}$ , and 90% of banana flour was  $119.19 \pm 4.61 \mu\text{m}$  (Figure 5). The cumulative particle size distribution is the percent distribution of the undersized particle. Thus, there is a large difference in the D10, D50, and D90 distribution of the total percent of particles in banana flour. The mean value of the particle size in banana flour was found to be  $60.75 \pm 1.99 \mu\text{m}$ . The finding was observed to be lower than the value ( $222.89 \mu\text{m}$ ) reported for commercial banana flour manufactured by Kunachia LLC, Davie, FL, USA [47]. The span value was  $2.17 \pm 0.05$ , which gives an idea of how far 10% and 90% are apart and normalize with the mid-point. The different drying techniques (oven drying and freeze drying), drying temperature, and grinding methods (ball mill, pulverizer, and blade grinder) may affect the particle size distribution and physicochemical properties [47, 48]. Convective drying triggers rapid desiccation of moisture and structural collapse, and furthermore, it varies due to a rise in drying temperature and hot air flow rate. In

TABLE 5: Characteristics of optimized green banana flour.

Properties	Content
<b>Physicochemical properties</b>	
Moisture (%)	9.99 ± 0.04
Protein (%)	1.23 ± 0.04
Fat (%)	1.79 ± 0.11
Crude fiber (%)	4.66 ± 0.04
Ash (%)	5.10 ± 0.04
Total carbohydrates (%)	77.25 ± 0.06
Acidity (% citric acid)	0.55 ± 0.03
TSS (%)	0.72 ± 0.00
pH	6.01 ± 0.00
<b>Flow properties</b>	
Angle of repose (°)	34.12 ± 0.61
Bulk density (g/cm <sup>3</sup> )	0.26 ± 0.00
Tapped density (g/cm <sup>3</sup> )	0.31 ± 0.00
Carr's index	16.51 ± 1.02
Hausner ratio	1.2 ± 0.01
Compressibility index	16.51 ± 1.02
<b>Functional properties</b>	
WAC (g/g)	5.19 ± 0.01
OAC (g/g)	1.58 ± 0.01
Solubility (g/g)	0.14 ± 0.02
<b>Particle size</b>	
D <sub>10</sub> (μm)	11.45 ± 0.17
D <sub>50</sub> (μm)	49.70 ± 2.01
D <sub>90</sub> (μm)	119.19 ± 4.61
Mean size (μm)	60.75 ± 1.99
Span	2.17 ± 0.05

The values given are the mean of the triplicate readings with the standard deviation.

the case of freeze-dried fruit flours, the quick sublimation of moisture from the surface of fruit slices contributes to a more porous structure and easy grinding that facilitates uniform particle size distribution. Khoozani et al. [48] reported that particle size uniformity is responsible for functional properties (WAC, OAC, wettability, and solubility), flowability in powder-based products, and mixing behaviours of flour in dough making and thermal properties.

The bulk density and tapped density of banana flour were  $0.26 \pm 0.00$  and  $0.31 \pm 0.00$  g/cm<sup>3</sup>. The good flowability in terms of CI and angle of repose was found at  $16.51 \pm 1.02$  and  $34.12 \pm 0.61^\circ$ , respectively (Table 5). HR and compressibility index of green banana flour were  $1.2 \pm 0.01$  and  $16.51 \pm 1.02$ , representing the intermediate flowability and fair compactness, respectively (Table 5). The bulk density of oven-dried green banana flour at 50, 80, and 110°C were reported to be 0.43, 0.53, and 0.66 g/cm<sup>3</sup> by Khoozani et al. [48]. The drying conditions are fruit specific. This is the reason behind optimizing drying conditions for the flour formulation with good flow properties, particle size, and functional properties. Therefore, green banana flour from optimized tray-drying conditions might have better application in product development.

**3.3.4. Thermal Properties.** DSC curves express the glass transition temperature (T<sub>g</sub>) and phase changes with respect to the change in temperature of banana flour. The thermogram of green banana flour showed gelatinization

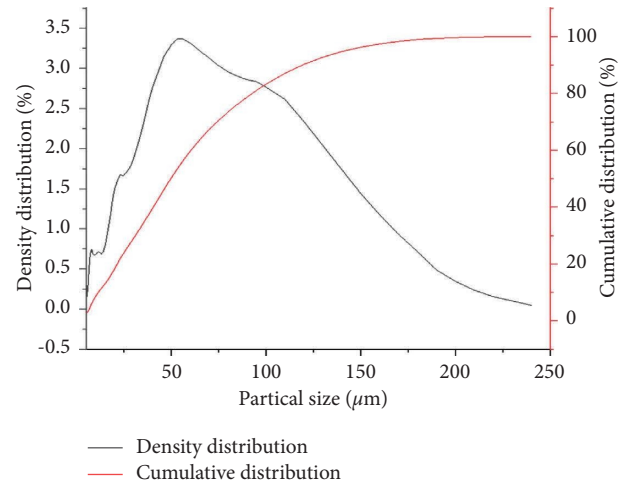


FIGURE 5: Particle size distribution (PSD) of optimized green banana flour.

onset, peak, end, and glass transition temperatures found as 84.4, 102.7, 106.8, and 93.8°C (Figure 6a). The peak temperature of five different varieties of green banana flour, namely, “Grand Naine”, “Monthan”, “Saba”, “Nandran”, and “Populu” flour, obtained after the hot air drying of banana slices at 55°C was found to be 91.01, 111.86, 98.82, 95.02, and 95.13°C, respectively [46]. The nonsignificant difference in peak temperature value of banana flour oven-dried at different temperatures of 50, 80, and 110°C was found to be 75.9, 74.60, and 75.86°C [49]. The higher melting temperature of different varieties of banana flour might be due to the high content of resistant starch and dietary fibers [49].

The enthalpy ( $\Delta H$ ) is the energy needed to disintegrate the molecular interaction within the starch structure throughout gelatinization. The  $\Delta H$  value of green banana flour was 12,222 J/g. The higher gelatinization temperature and enthalpy value indicate a good arrangement of starch molecules with higher amylopectin [50]. The specific heat of banana flour was 63.14 J/g (°K). The mass change/loss in weight of the sample with temperature ramp showed the thermal decomposition of the sample, which was determined by TGA (Figure 6b). In the first step, the mass loss (6.39%) was probably due to the dehydration and loss of volatile compounds in green banana flour at 120°C. The maximum mass loss temperature and decomposition temperature of green banana flour were 70 and 292°C, respectively. Between the first and second stages of mass loss showed the thermal stability period, there was no loss in mass occurred (120–220°C). During the second stage, mass loss occurs at 220–361 °C, showing maximum mass loss (52.09%) and minimum derivative value. These showed that the depolymerization of the carbohydrate chain results in the decomposition of amylose and amylopectin and released gaseous compounds [32, 51]. The present mass loss value was lower than the value reported for the rejected plantain fruit, which was  $10.79 \pm 0.04$  and  $59.3 \pm 0.1\%$  for first- and second-stage mass loss [51]. Similarly, Cordoba et al. [32]

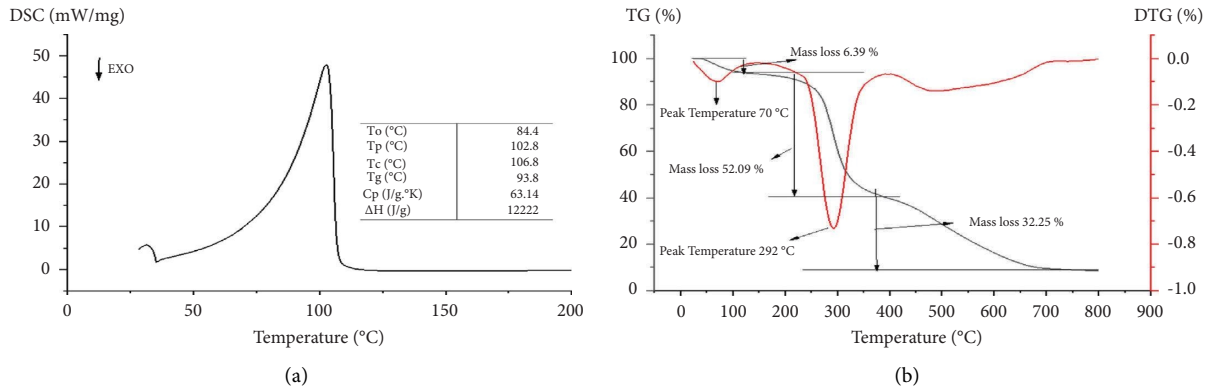


FIGURE 6: Thermal analysis of green banana flour: (a) Differential scanning calorimetric (DSC). (b) Thermogravimetric analysis (TGA) and differential thermogravimetric analysis (DTGA).

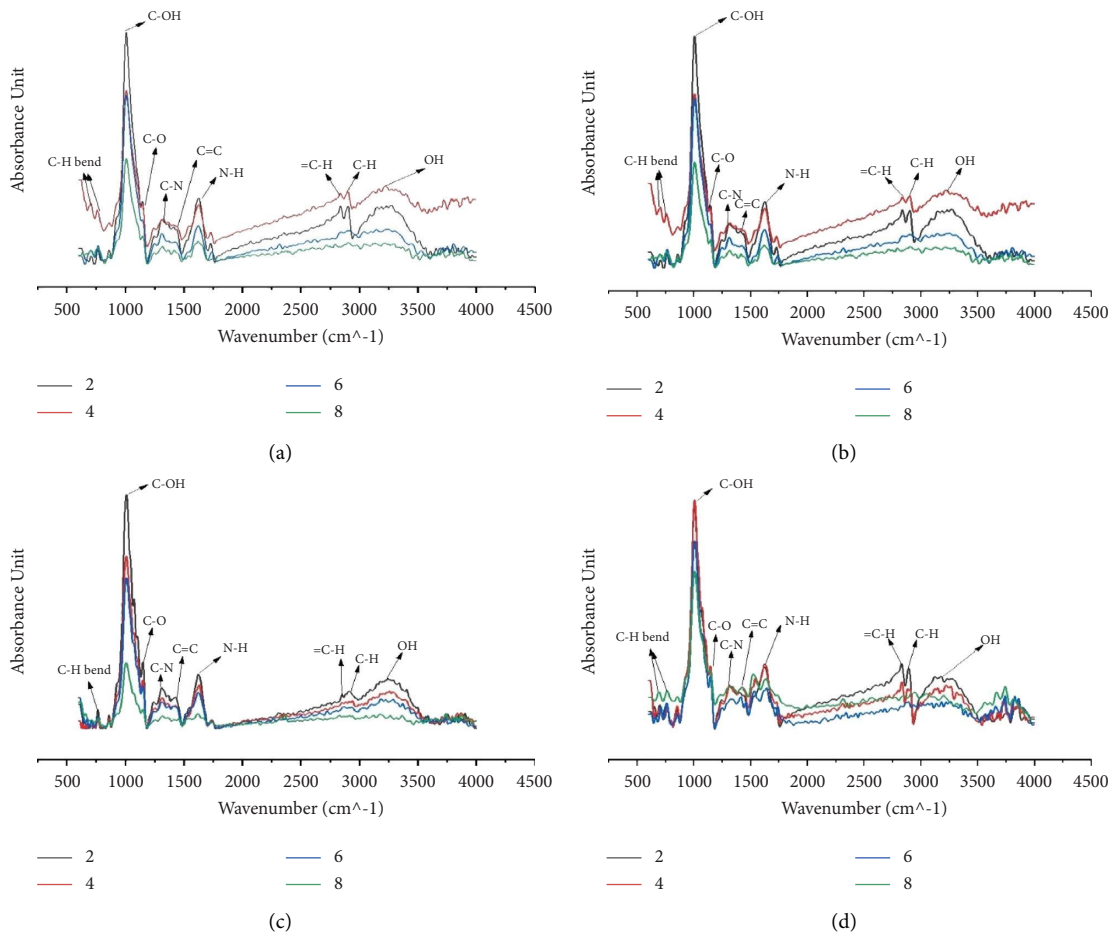


FIGURE 7: Fourier transform infrared spectrophotometer (FTIR) spectrum analysis of green banana flour dried at 50°C (a), 60°C (b), 70°C (c), and 80°C (d).

reported a higher mass loss of green bananas in the first (12.65°C) and second stage of decomposition (66.69–68.88°C). These differences in thermal properties might be due to the composition of the biomolecule in raw material, drying techniques, and the maturity stage of fruit [51]. The third stage loss in mass was 32.25% at

361–660°C. Further yields the lowest residual mass at the end of decomposition (8.57%). The difference in crude fiber, ash, and protein content is responsible for higher residual mass [52]. This flour can be used in the application of soup sausages to maintain the higher temperature stability of gel.

**3.3.5. Fourier Transform Infrared Spectroscopy (FTIR).** The main FTIR spectra of the tray-dried flour at different temperatures and thicknesses were 710, 766, 1008, 1146, 1321, 1436, 1623, 2830.90, 2945.81, and 32433, respectively (Figures 7(a)–7(d)). The stronger intensity of broadband between 3300 and 3400  $\text{cm}^{-1}$  showed the symmetric and asymmetric stretching of the O–H group of hydrogen bonds. This is strongly evidenced by the presence of phenolic compounds [24, 46].

The peak at 2850–3000 was related to the stretching vibration of the C–H group of protein and polysaccharides [24]. The variable intensity between 2820 and 2850  $\text{cm}^{-1}$  showed the existence of =C–H stretching of the aldehyde group. The amide I band was found between 1550 and 1640  $\text{cm}^{-1}$  showing the bending of the N–H group, indicating the presence of an amide group of protein. The medium-weak band in between 1400 and 1600  $\text{cm}^{-1}$  showed the presence of an aromatic (C=C) compound of flour. The peak at 1321  $\text{cm}^{-1}$  related to stretching of the C–N bond, indicating the presence of aromatic amide group (amide III) [24]. The peak is located in the region between 400 and 1200  $\text{cm}^{-1}$  that originates mainly from the vibration of the functional group of carbohydrates (Figure 7). In this region, the bands at 1146  $\text{cm}^{-1}$  showed the stretching of the C–O group of carbohydrate polymer; the band at 1008  $\text{cm}^{-1}$  was attributed to the stretching of the COH bond associated with the crystalline and amorphous structure of banana flour containing starch [53]. The absorption band at 766 and 710  $\text{cm}^{-1}$  showed the bending of the C–H group of monosubstituted and O-di substituted aromatic compound present in flour. No change in the chemical group was observed during banana drying, but the intensity and accurate position differed with different drying temperatures and slice thicknesses (Figure 7). Thus, the tray-dried green banana flour exhibited the presence of phytochemicals with varying compositions, as verified by the analysis of total phenolic and flavonoid content.

## 4. Conclusions

The convective tray-drying conditions for green banana slices were successfully optimized at a drying temperature of 50°C and slice thickness of 4.5 mm. The experimental responses showed maximum  $L^*$  (84.06),  $C^*$  (13.73), and  $h^o$  (83.53) values and minimum TPC (89.22 mg GAE/100 g) and TFC (3.10 mg quercetin/100 g) losses in dried green banana slices. The minimum changes in color values and phytochemical compound losses in dried green banana flour were observed under the optimized conditions. Despite this, lower  $a_w$  (0.25) of optimized banana flour facilitated positively to the flour quality during processing as well as it might be led to long-term preservation of banana flour. However, low water activity inhibits the several biochemical reactions. The lower  $a_w$  of banana flour makes it shelf-stable from nonmicrobial reactions. The results obtained by various other researchers during drying of green bananas under different drying conditions are compared in Table 4. Thuwapanichayanan et al. [12] who had dried the banana slices (3 mm) at 70–100°C reported the maximum  $h^o$  79.35 at 70°C

compared to those dried at 90 ( $h^o$  78.59) and 100°C ( $h^o$  73.16). Olusegun-Omolola et al. [13] reported that the significant difference in  $h^o$  values of banana flour (74.60 and 68.99°) obtained at 47.56 and 68.99°C might be due to the oxidation and degradation of overall color with a rise in drying temperature. The obtained findings of water activity agreed with those of Savas [34]. It reported the lowest  $a_w$  0.36 of dried sweet potato slices at an optimized drying condition of 75°C for 4.42 h with a sample slice thickness of 6 mm, which is higher than the present study reporting  $a_w$  value at an optimized condition. Erbay and Icier [40] reported an increased percent loss of TPC of convectively dried olive leaves (8.13–37.25%) at 40–60°C with air velocity of 0.5–1.5 m/s and process time of 240–480 min, which was higher than present study's TPC of the banana slice at an optimized condition. Hence, in total, the drying conditions optimized in this study can be observed to be better than the previous studies.

The green banana flour obtained after pulverizing the dried slices at optimized conditions was lower in fat and protein and higher in total carbohydrate and had good flowability, WAC, and OAC. The FTIR analysis showed intensity and accurate position of the functional group differed with different drying temperatures and slice thicknesses. Furthermore, the DSC and TGA analysis revealed green banana flour's maximum gelatinization, dehydration, and decomposition temperature and these might be due to the compositional changes in banana (maximum starch and dietary fiber content). The green banana flour obtained in this study can be useful for numerous applications in food and nonfood processing industries such as to develop high temperature stable gel, thickening, encapsulating agent, and binder in tablet formulation [21, 26]

## Abbreviations

$\rho_b$ :	Bulk density
$a_w$ :	Water activity
$R^2$ :	Coefficient of determination
$V_c$ :	Compact volume
$V_p$ :	Porous volume
$\rho_t$ :	Tapped density
$\mu\text{L}$ :	Microliter
$C^*$ :	Chroma
CV:	Coefficient of variance
CI:	Carr index
DSC:	Differential scanning calorimetry
DTGA:	Differential thermogravimetric
FTIR:	Fourier transform infrared spectrophotometer
$\text{g}/\text{cm}^3$ :	Gram per cubic centimetre
$\text{g}/\text{g}$ :	Gram per gram
GAE:	Gallic acid equivalents
h:	Height
$h^o$ :	Hue angle
HR:	Hausner ratio
$L^*$ :	Lightness
mg:	Milligram
mm:	Millimetre

N: Normality  
 OAC: Oil absorption capacity  
 QE: Quercetin equivalent  
 r: Radius  
 RSM: Response surface methodology  
 TA: Titratable acidity  
 TFC: Total flavonoid content  
 TGA: Thermogravimetric analysis  
 TPC: Total phenolics content  
 TSS: Total soluble solids  
 WAC: Water absorption capacity  
 $\alpha$ : Angle of repose  
 $\mu\text{m}$ : Micrometre.

## Data Availability

Data will be made available upon request to the corresponding author.

## Conflicts of Interest

The authors declare no conflicts of interest.

## Authors' Contributions

Writing of the original draft, editing, software provision, conceptualization, methodology, formal analysis, and validation were carried out by MK. Conceptualization, supervision, validation, methodology, investigation, and reviewing were performed by AS. Review and editing were performed by SP. Software provision and review and editing were performed by SVS. Review and editing were done by AC. All authors have read and agreed to the published version of manuscript.

## Acknowledgments

The authors express their gratitude to NIFTEM administration, Kundli, Sonipat (India), for providing the necessary infrastructure to do this research work. Also, the authors would like to thank the lab staff of Food Science and Technology Department Lab and the Central Instrumentation Lab, NIFTEM, for their assistance in providing the resources. This research work was funded by the National Institute of Food Technology Entrepreneurship and Management, Kundli, under the Ph.D. research grant no. Ph.D./17-18/7/175.

## References

- [1] S. Alzate Acevedo, A. J. Díaz Carrillo, E. Flórez-López, and C. D. Grande-Tovar, "Recovery of banana waste-loss from production and processing: a contribution to a circular economy," *Molecules*, vol. 26, no. 17, pp. 5282–5312, 2021.
- [2] ABC Fruits, *Banana Varieties, Production, and Season in India*, 2021, <https://www.abcfruits.net/banana-varieties-production-and-season-in-india/>.
- [3] J. J. Bhaskar, S. Mahadevamma, N. D. Chilkunda, and P. V. Salimath, "Banana (*Musa* sp. var. *Elakki Bale*) flower and pseudostem: dietary fiber and associated antioxidant capacity," *Journal of Agricultural and Food Chemistry*, vol. 60, no. 1, pp. 427–432, 2012.
- [4] L. Rajapaksha, D. C. Gunathilake, S. M. Pathirana, and T. Fernando, "Reducing post-harvest losses in fruits and vegetables for ensuring food security - case of Sri Lanka," *MOJ Food Processing & Technology*, vol. 9, no. 1, pp. 7–16, 2021.
- [5] *Poor Storage Leads to 50 Per Cent Banana Losses after Harvest*, 2021, <https://timesofindia.indiatimes.com/city/trichy/half-of-post-harvest-banana-loss-caused-by-poor-storage-system/articleshow/74261788.cms>.
- [6] V. Singh, M. Hedayetullah, P. Zaman, and J. Meher, "Post-harvest technology of fruits and vegetables: an overview," *Journal of Postharvest Technology*, vol. 2, no. 2, pp. 124–135, 2014.
- [7] P. Powthong, B. Jantrapanukorn, P. Suntornthiticharoen, and K. Laohaphatanalert, "Study of prebiotic properties of selected banana species in Thailand," *Journal of Food Science & Technology*, vol. 57, no. 7, pp. 2490–2500, 2020.
- [8] C. Phungamngoen, N. Chiewchan, and S. Devahastin, "Thermal resistance of *Salmonella enterica* serovar Anatum on cabbage surfaces during drying: effects of drying methods and conditions," *International Journal of Food Microbiology*, vol. 147, no. 2, pp. 127–133, 2011.
- [9] R. Zhao and T. Gao, "Research progress of hot air drying technology for fruits and vegetables," *Advance Journal of Food Science and Technology*, vol. 10, no. 3, pp. 160–166, 2016.
- [10] H. Bozkir, "Effects of hot air, vacuum infrared, and vacuum microwave dryers on the drying kinetics and quality characteristics of orange slices," *Journal of Food Process Engineering*, vol. 43, no. 10, Article ID e13485, 2020.
- [11] P. J. Etim, A. B. Eke, K. J. Simonyan, K. C. Umani, and S. Udo, "Optimization of solar drying process parameters of cooking banana using response surface methodology," *Scientific African*, vol. 13, Article ID e00964, 2021.
- [12] R. Thuwapanichayanan, S. Prachayawarakorn, J. Kunwisawa, and S. Soponronnarit, "Determination of effective moisture diffusivity and assessment of quality attributes of banana slices during drying," *LWT--Food Science and Technology*, vol. 44, no. 6, pp. 1502–1510, 2011.
- [13] A. Olusegun-Omolola, A. L. Obiefuna-Jideani, P. Francis-Kapila, and V. Adaora-Jideani, "Optimization of oven drying conditions of banana (*Musa* spp., AAA Group, cv. 'Luvhele' and 'Mabonde') using response surface methodology," *Agrociencia*, vol. 52, no. 4, pp. 539–551, 2018.
- [14] L. T. K. Do, L. T. K. Vu, D. T. A. Phan, and N. T. Dzung, "Mathematical modeling and optimization of low-temperature vacuum drying for banana," *Carpathian Journal of Food Science and Technology*, vol. 13, no. 4, pp. 47–61, 2021.
- [15] A. O. Omolola, A. I. O. Jideani, P. F. Kapila, and V. A. Jideani, "Optimization of microwave drying conditions of two banana varieties using response surface methodology," *Food Science and Technology*, vol. 35, no. 3, pp. 438–444, 2015.
- [16] R. F. Zabalaga, C. I. La Fuente, and C. C. Tadini, "Experimental determination of thermophysical properties of unripe banana slices (*Musa cavendishii*) during convective drying," *Journal of Food Engineering*, vol. 187, pp. 62–69, 2016.
- [17] R. F. Zabalaga and S. C. Carballo, "Convective drying and water adsorption behavior of unripe banana: mathematical modeling," *Journal of Food Processing and Preservation*, vol. 39, no. 6, pp. 1334–1341, 2015.
- [18] A. Calín-Sánchez, L. Lipan, M. Cano-Lamadrid et al., "Comparison of traditional and novel drying techniques and its effect on quality of fruits, vegetables and aromatic herbs," *Foods*, vol. 9, no. 9, pp. 1261–1288, 2020.

- [19] Y. Kumar, V. S. Sharanagat, L. Singh, and P. K. Nema, "Convective drying of spine gourd (*Momordica dioica*): effect of ultrasound pre-treatment on drying characteristics, color, and texture attributes," *Journal of Food Processing and Preservation*, vol. 44, no. 9, pp. 14639–14650, 2020.
- [20] M. G. Kamble, A. Singh, V. Mishra, M. Meghwal, and P. K. Prabhakar, "Mass and surface modelling of green plantain banana fruit based on physical characteristics," *Computers and Electronics in Agriculture*, vol. 186, Article ID 106194, 2021.
- [21] M. G. Kamble, A. Singh, P. Kumar Prabhakar, M. Meghwal, S. Veer Singh, and A. V. Chinchkar, "Effect of high shear homogenization on quality characteristics of bael fruit pulp," *Food Quality and Safety*, vol. 6, 2022.
- [22] S. Padhi and M. Dwivedi, "Physico-chemical, structural, functional and powder flow properties of unripe green banana flour after the application of Refractance window drying," *Future Foods*, vol. 5, Article ID 100101, 2022.
- [23] AOAC, *Official Methods of Analysis*, Association of Official Analytical Chemists International, Gaithersburg, MD, 2006.
- [24] T. J. Gutiérrez, "Plantain flours as potential raw materials for the development of gluten-free functional foods," *Carbohydrate Polymers*, vol. 202, pp. 265–279, 2018.
- [25] L. M. Rayo, L. Chaguri e Carvalho, F. A. H. Sardá, G. C. Dacanal, E. W. Menezes, and C. C. Tadini, "Production of instant green banana flour (*Musa cavendishii*, var. *Nanicão*) by a pulsed-fluidized bed agglomeration," *LWT - Food Science and Technology*, vol. 63, no. 1, pp. 461–469, 2015.
- [26] S. V. Singh, R. Singh, A. Singh et al., "Optimization of enzymatic hydrolysis parameters for sapodilla fruit (*Manilkara achras* L.) juice extraction," *Journal of Food Processing and Preservation*, vol. 46, no. 3, 2022.
- [27] K. A. Taiwo and R. T. Babalola, "Studies on the drying kinetics and rehydration capacities of Cardaba banana compared to plantain slices," *Open Agriculture*, vol. 3, no. 1, pp. 57–71, 2018.
- [28] M. S. Anuar, S. M. Tahir, M. I. Najeeb, and S. Ahmad, "Banana (*Musa acuminata*) peel drying and powder characteristics obtained through shade and microwave drying processes," *Advances in Materials and Processing Technologies*, vol. 5, no. 2, pp. 181–190, 2019.
- [29] C. Turchiuli, Z. Eloualia, N. El Mansouri, and E. Dumoulin, "Fluidised bed agglomeration: agglomerates shape and end-use properties," *Powder Technology*, vol. 157, no. 1-3, pp. 168–175, 2005.
- [30] H. Mirhosseini and B. T. Amid, "Effect of different drying techniques on flowability characteristics and chemical properties of natural carbohydrate-protein gum from durian fruit seed," *Chemistry Central Journal*, vol. 7, no. 1, pp. 1–14, 2013.
- [31] J. Ahmed, L. Thomas, and R. Khashawi, "Influence of hot-air drying and freeze-drying on functional, rheological, structural and dielectric properties of green banana flour and dispersions," *Food Hydrocolloids*, vol. 99, pp. 105331–105341, 2020.
- [32] L. d. P. Cordoba, R. G. da Silva, D. d. S. Gomes, E. Schnitzler, and N. Waszczynskyj, "Brazilian green banana," *Journal of Thermal Analysis and Calorimetry*, vol. 134, no. 3, pp. 2065–2073, 2018.
- [33] G. J. Fadimu, L. O. Sanni, A. Adebawale et al., "Effect of drying methods on the chemical composition, color, functional and pasting properties of plantain (*Musa parasidiaca*) flour," *Croatian Journal of Food Technology, Biotechnology and Nutrition*, vol. 13, no. 1-2, pp. 38–43, 2018.
- [34] E. Savas, "The modelling of convective drying variables' effects on the functional properties of sliced sweet potatoes," *Foods*, vol. 11, no. 5, p. 741, 2022.
- [35] D. Kohli, P. S. Champawat, S. K. Jain, V. D. Mudgal, and N. C. Shahi, "Mathematical modelling for drying kinetics of asparagus roots (*Asparagus racemosus* L.) and determination of energy consumption," *Biointerface Research in Applied Chemistry*, vol. 12, no. 3, pp. 3572–3589, 2022.
- [36] W. L. Kerr and A. Varner, "Chemical and physical properties of vacuum-dried red beetroot (*Beta vulgaris*) powders compared to other drying methods," *Drying Technology*, vol. 38, no. 9, pp. 1165–1174, 2019.
- [37] X. Fu, S. Cheng, Y. Liao et al., "Comparative analysis of pigments in red and yellow banana fruit," *Food Chemistry*, vol. 239, pp. 1009–1018, 2018.
- [38] E. O. Anajekwu, B. Maziya-Dixon, R. Akinoso, W. Awoyale, and E. O. Alamu, "Physicochemical properties and total carotenoid content of high-quality unripe plantain flour from varieties of hybrid plantain cultivars," *Journal of Chemistry*, vol. 2020, pp. 1–7, 2020.
- [39] J. R. d. J. Junqueira, J. L. G. Corrêa, H. M. de Oliveira, R. Ivo SoaresAvelar, and L. A. Salles Pio, "Convective drying of cape gooseberry fruits: effect of pre-treatments on kinetics and quality parameters," *LWT--Food Science and Technology*, vol. 82, pp. 404–410, 2017.
- [40] Z. Erbay and F. Icier, "Optimization of hot air drying of olive leaves using response surface methodology," *Journal of Food Engineering*, vol. 91, no. 4, pp. 533–541, 2009.
- [41] B. Önal, G. Adiletta, A. Crescitelli, M. Di Matteo, and P. Russo, "Optimization of hot air drying temperature combined with pre-treatment to improve physico-chemical and nutritional quality of "Annurca" apple," *Food and Bio-products Processing*, vol. 115, pp. 87–99, 2019.
- [42] K. S. Srikanth, V. S. Sharanagat, Y. Kumar et al., "Influence of convective hot air drying on physico-functional, thermo-pasting and antioxidant properties of elephant foot yam powder (*Amorphophallus paeoniifolius*)," *Journal of Food Science & Technology*, pp. 1–10, 2021.
- [43] T. M. Rababah, M. Alhamad, M. Al-Mahasneh et al., "Effects of drying process on total phenolics, antioxidant activity and flavonoid contents of common mediterranean herbs," *International Journal of Agricultural and Biological Engineering*, vol. 8, no. 2, pp. 145–150, 2015.
- [44] A. K. Jha and N. Sit, "Drying characteristics and kinetics of colour change and degradation of phytochemicals and antioxidant activity during convective drying of deseeded *Terminalia chebula* fruit," *Journal of Food Measurement and Characterization*, vol. 14, no. 4, pp. 2067–2077, 2020.
- [45] S. R. Fatemeh, R. Saifullah, F. M. A. Abbas, and M. E. Azhar, "Total phenolics, flavonoids and antioxidant activity of banana pulp and peel flours: influence of variety and stage of ripeness," *International Food Research Journal*, vol. 19, no. 3, pp. 1041–1046, 2012.
- [46] P. S. Kumar, A. Saravanan, N. Sheeba, and S. Uma, "Structural, functional characterization and physicochemical properties of green banana flour from dessert and plantain bananas (*Musa* spp.)," *LWT - Food Science and Technology*, vol. 116, pp. 108524–108536, 2019.
- [47] S. Huang, M. M. Martinez, and B. M. Bohrer, "The compositional and functional attributes of commercial flours from tropical fruits (breadfruit and banana)," *Foods*, vol. 8, no. 11, pp. 586–601, 2019.
- [48] A. Amini Khoozani, J. Birch, and A. E. D. A. Bekhit, "Textural properties and characteristics of whole green banana flour

- produced by air-oven and freeze-drying processing,” *Journal of Food Measurement and Characterization*, vol. 14, no. 3, pp. 1533–1542, 2020.
- [49] A. A. Khoozani, A. E. D. A. Bekhit, and J. Birch, “Effects of different drying conditions on the starch content, thermal properties and some of the physicochemical parameters of whole green banana flour,” *International Journal of Biological Macromolecules*, vol. 130, pp. 938–946, 2019.
- [50] R. G. Utrilla-Coello, M. E. Rodríguez-Huezo, H. Carrillo-Navas, C. Hernández-Jaimes, E. J. Vernon-Carter, and J. Alvarez-Ramirez, “In vitro digestibility, physicochemical, thermal and rheological properties of banana starches,” *Carbohydrate Polymers*, vol. 101, pp. 154–162, 2014.
- [51] J. A. Gómez, E. Pino-Hernández, L. Abrunhosa et al., “Valorisation of rejected unripe plantain fruits of *Musa* AAB Simmonds: from nutritional characterisation to the conceptual process design for prebiotic Production,” *Food & Function*, vol. 12, no. 7, pp. 3009–3021, 2021.
- [52] N. A. Sagar, A. Khar, A. Tarafdar, A. Tarafdar, and S. Pareek, “Physicochemical and thermal characteristics of onion skin from fifteen Indian cultivars for possible food applications,” *Journal of Food Quality*, vol. 2021, pp. 1–11, 2021.
- [53] D. M. Fan, W. Ma, L. Wang et al., “Determination of structural changes in microwaved rice starch using Fourier Transform Infrared and Raman Spectroscopy,” *Starch Staerke*, vol. 64, no. 8, pp. 598–606, 2012.